Gold-titania interface toughening and thermal conductance enhancement using an organophosphonate nanolayer

Philippe K. Chow,[1] Y. Cardona Quintero,[2] Peter O'Brien,[1] P. Hubert Mutin,[3] Michael Lane,[4] R. Ramprasad,[2] and Ganpati Ramanath[1,a)]
[1]Rensselaer Polytechnic Institute, Department of Materials Science and Engineering, Troy, New York 12180, USA
[2]Materials Science and Engineering, University of Connecticut, Storrs, Connectict 06269, USA
[3]Institut Charles Gerhardt Montpellier, UMR 5253 CNRS-UM2-ENSCM-UM1, Université Montpellier 2, CC 1701, Place Eugène Bataillon, 34095 Montpellier Cedex 5, France
[4]Chemistry Department, Emory and Henry College, Emory, Virginia 24327, USA

(Received 8 February 2013; accepted 4 May 2013; published online 21 May 2013)

We demonstrate that a mercaptan-terminated organophosphonate nanolayer at gold-titania interfaces can give rise to two- to three-fold enhancement in the interfacial fracture toughness and thermal conductance. Electron spectroscopy reveals that interfacial delamination occurs at the metal-molecule interface near the gold-sulfur bonds, consistent with density functional theory calculations of bond energies. Qualitative correlation between interfacial fracture toughness and bond energies suggest that organophosphonate nanolayers are resilient to humidity-induced degradation. These results, and the versatility of organophosphonates as surface functionalization agents for technologically relevant materials, unlock uncharted avenues for molecular engineering of interfaces in materials and devices for a variety of applications. © *2013 AIP Publishing LLC*. [http://dx.doi.org/10.1063/1.4807436]

A number of composite materials[1] and emerging technologies in electronics,[2,3] catalysis,[4] and biomedicine[5] strongly depend on metal-ceramic interfaces with tailored electronic and thermal properties, and thermomechanical stability. An ultrathin nanoglue layer[6] is often necessary to promote interfacial adhesion and inhibit chemical intermixing[7] to preserve the functionality of the materials constituting the interface. Prior work has shown that nanomolecular layers (NMLs) can meet both these exacting requirements. For instance, the fracture toughness of copper-silica interfaces can be enhanced several-fold by introducing a strongly bonding NML at the interface[6] while hindering copper diffusion that leads to the electrical breakdown of silica.[8] This approach has the potential to be transmuted to other metal-ceramic systems for a wider set of applications by using NMLs with different termini, but is yet to be fully explored and exploited. Example opportunities include aligning the work function of metal electrodes with silicon band edges[2] across a high dielectric permittivity gate oxide (e.g., Ta_2O_5, HfO_2) in metal-oxide-semiconductor transistors,[9,10] manipulating electron transfer characteristics at nanocatalyst-support (e.g., Au-oxide) interfaces,[4] tailoring interfaces of inorganic implant biomaterials (e.g., Ti),[5] and tuning interfacial thermal conductance.[11]

Here, we demonstrate a 2.5-fold increase in the fracture toughness and a 3-fold enhancement in interfacial thermal conductance of gold-titania interface by incorporating a mercaptan-terminated organophosphonate NML at the interface. Electron spectroscopy and density functional theory (DFT) calculations of bond energies show that interface delamination occurs at the Au-NML interface in the vicinity of the Au-S bond. Our results also show the resilience of organophosphonate NMLs against moisture-induced corrosion. We chose a mercaptan-terminated organophosphonate, namely, 12-mercaptododecyl phosphonic acid (MDPA), because mercaptan termini bond strongly with noble metals[6] and the phosphonate moiety forms oxygen-mediated covalent bridges with technologically important oxide materials such as hafnia,[13] titania,[14] and zirconia.[15] Our results, and the versatility of phosphonates for use in bioseparation,[15] dye-sensitized solar cells,[16] and nanocomposites,[1,17] unlock uncharted avenues for molecular engineering of interfaces in materials and devices for a variety of applications.

We deposited a 100-nm-thick Ti film by sputter deposition in a 7 mTorr argon plasma on *n*-type Si(001) substrates capped with an 85-nm-thick silica layer. The substrates were successively washed in methanol, acetone, and isopropanol, and dried with nitrogen immediately prior to the deposition. The metal film was fully oxidized by rapid thermal annealing to 700 °C for 60 s in flowing oxygen. X-ray diffraction and scanning electron microscopy reveal that the titanium oxide film had the rutile structure, with an average grain size of ∼100 nm and a 10 nm rms roughness. A MDPA NML was assembled onto the titania surface by immersing the titania-coated Si wafers for 48 h in a N_2-purged 1 mM ethanolic MDPA solution at room temperature. Physisorbed MDPA was removed by sonication in methanol, acetone, and isopropanol for 30 s each, followed by drying with ultrahigh purity nitrogen. We also prepared some samples without the rinsing step to assess the effect of remnant physisorbed MDPA (phys-MDPA) on interfacial properties. The MDPA/TiO_2/SiO_2/Si structures were loaded into the e-beam evaporator within 5 min for subsequent metal deposition to minimize NML exposure.

We fabricated dummy-Si/epoxy/Ti/Au/MDPA/TiO_2/SiO_2/Si structures (Fig. 1(c) inset) to determine the fracture

a)Author to whom correspondence should be addressed. Electronic mail: Ramanath@rpi.edu

 © 2013 AIP Publishing LLC

Downloaded 13 Jun 2013 to 137.99.20.247. This article is copyrighted as indicated in the abstract. Reuse of AIP content is subject to the terms at: http://apl.aip.org/about/rights_and_permissions

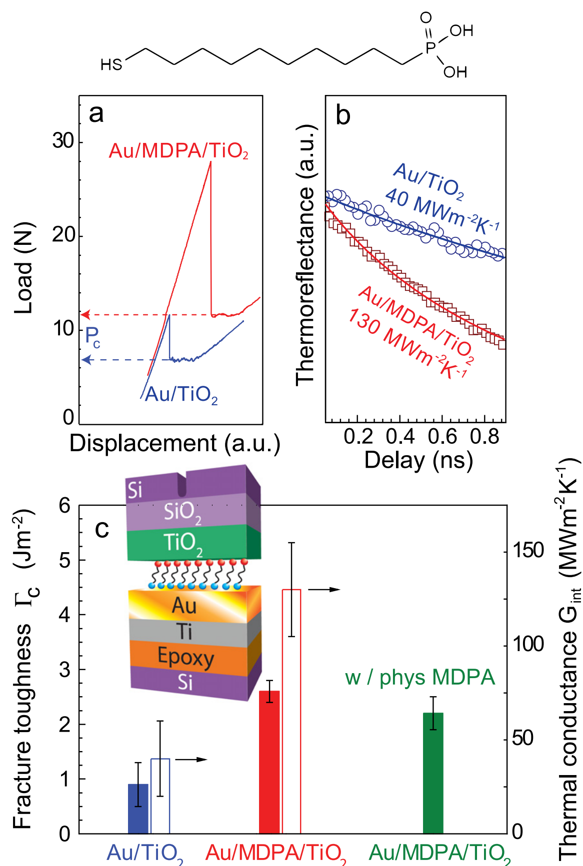

FIG. 1. (a) Load-displacement curves and (b) time-domain thermoreflectance decay profiles for structures with pristine Au/TiO_2 and $Au/MDPA/TiO_2$ interfaces. The solid lines represent the best-fit thermal decay profiles from a one-dimensional heat conduction model. (c) The fracture toughness (filled, left axis) and interface thermal conductance (unfilled, right axis) for pristine Au/TiO_2 and $Au/MDPA/TiO_2$ interfaces. Fracture toughness of MDPA-treated interfaces with remnant physisorbed MDPA is also shown.

toughness Γ_c of the weakest interface by four-point bend tests[18] carried out at a 0.03 μm s^{-1} strain rate. A 50-nm-thick Au film was deposited on pristine titania and on MDPA-treated titania by e-beam evaporation. Additionally, a 50-nm-thick Ti layer was deposited without vacuum break to prevent delamination at the weak Au-epoxy interface.[19] The $Ti/Au/MDPA/TiO_2/SiO_2/Si$ stacks were bonded to a dummy Si wafer using a high-temperature curing epoxy, and diced into 40 mm × 5.6 mm beams. A 625-μm-deep notch was carefully machined into the host Si wafer to initiate delamination. Steady-state interfacial delamination occurs when a crack from the notch reaches the weakest interface and propagates along the interface at a critical plateau load in the load-displacement curve. Γ_c was determined from this plateau load using a well-documented procedure described elsewhere.[20] Within about 5 min of delamination, we loaded the fracture pieces into a PHI 5400 X-ray photoelectron spectroscopy (XPS) chamber equipped with an Al Kα source. Core-level spectra were acquired from the fracture surfaces through survey and high resolution scans at 187.5 and 23.5 eV pass energies, respectively. The 285.0 eV adventitious C 1s peak and/or the 84 eV Au $4f_{7/2}$ peak were used for charging corrections. The sample surface-to-detector takeoff angle was set at $\theta_{sd} = 45°$ unless otherwise noted.

DFT computations were carried out to calculate the cleavage energies at different locations of the MDPA-functionalized $Au\text{-}TiO_2$ interface, using the Vienna *ab initio* simulation package code[23] with the Perdew-Burke-Ernzerhof generalized gradient approximation[24] and the projector-augmented wave[25] approach. The MDPA was bonded to TiO_2 in the bidentate configuration between Ti and the O atoms of the phosphonic acid, and to Au by an Au-S bond. We examined $Au\text{-}TiO_2$ interfaces with two different MDPA coverages. The higher coverage was simulated by matching a $(2 \times \sqrt{3})$ Au (111) slab to conform to a (1×2) TiO_2 (110), while the lower coverage was obtained by matching a $(4 \times 2\sqrt{3})$ Au (111) slab to a (2×4) TiO_2 (110).

We determined interfacial thermal conductance G_{int} from thermoreflectance decay profiles obtained from $Au/MDPA/TiO_2$ structures using time-domain thermoreflectometry.[11] Briefly, 5d electrons from the gold film surface are excited to above the Fermi level with a 800-nm wavelength 100 fs pump laser pulse.[21] The de-excitation of these electrons via phonon scattering heats the metal, and the heat is dissipated across the metal-ceramic interface. The temperature decay profile across the interface is obtained by tracking the temperature-dependent metal surface reflectance at different time delays using a separate 600-nm-wavelength 100 fs probe laser. G_{int} is extracted by fitting the thermoreflectance decay profile with a one-dimensional heat conduction model.

Load-displacement curves from test structures with MDPA-treated interfaces exhibit a significantly higher toughness than the untreated pristine interfaces (Figs. 1(a)–1(c)). $Au/MDPA/TiO_2$ interfaces show $\Gamma_c^{MDPA} = 2.6 \pm 0.2$ Jm^{-2}, which is more than twofold the $\Gamma_c^{baseline} = 0.9 \pm 0.4$ Jm^{-2} for pristine Au/TiO_2 interfaces. Mechanical tests of $Au/MDPA/TiO_2$ interfaces with remnant physisorbed MDPA, prepared by omitting the rinsing step, yield a comparable $\Gamma_c^{phys-MDPA} = 2.2 \pm 0.3$ Jm^{-2}. Each fracture toughness value is an average of six experiments. The uncertainties denote sample-to-sample variation. Comparison of thermal decay profiles across Au/TiO_2 interfaces with and without MDPA (Fig. 1(c)) reveals more than threefold enhancement in G_{int} upon introducing the MDPA NML. The best-fit thermal model yields $G_{int}^{MDPA} = 130$ MW m^{-2} K^{-1} and $G_{int}^{baseline} = 40$ MW m^{-2} K^{-1}, respectively. Thus, MDPA functionalization of Au/TiO_2 interfaces enhances both Γ_c and G_{int}.

Core-level spectra obtained from the fracture surfaces (Fig. 2(a)) provide insights into the atomistic mechanism of $Au/MDPA/TiO_2$ interface toughening. Titania fracture surfaces show sulfur and phosphorous signatures similar to that seen in as-prepared MDPA NMLs on TiO_2. The broad S $2p_{3/2}$ sub-band at 163.4 eV stems from unbound thiols and disulfides, while the 169.6 eV sub-band stems from sulfonate moieties[22] likely formed during mechanical testing in air and brief air-exposure prior to XPS. The P 2p band from the titania fracture surface is observed at a lower binding energy than in untethered MDPA, indicative of MDPA anchoring to titania via phosphonic acid moieties,[12] which is also supported by the decrease in the P 2p:S 2p integrated intensity ratio I_P/I_S with decreasing take-off angle θ_{sd} (Fig. 2(b)). Neither phosphorous nor sulfur is detectable on the Au fracture surface, indicating that delamination occurs by Au-S bond scission at the Au/MDPA interface. While P-O-Ti bonds are clearly stronger, both Au-S and P-O-Ti bonds at Au/MDPA and $MDPA/TiO_2$ interfaces, respectively, are

Downloaded 13 Jun 2013 to 137.99.20.247. This article is copyrighted as indicated in the abstract. Reuse of AIP content is subject to the terms at: http://apl.aip.org/about/rights_and_permissions

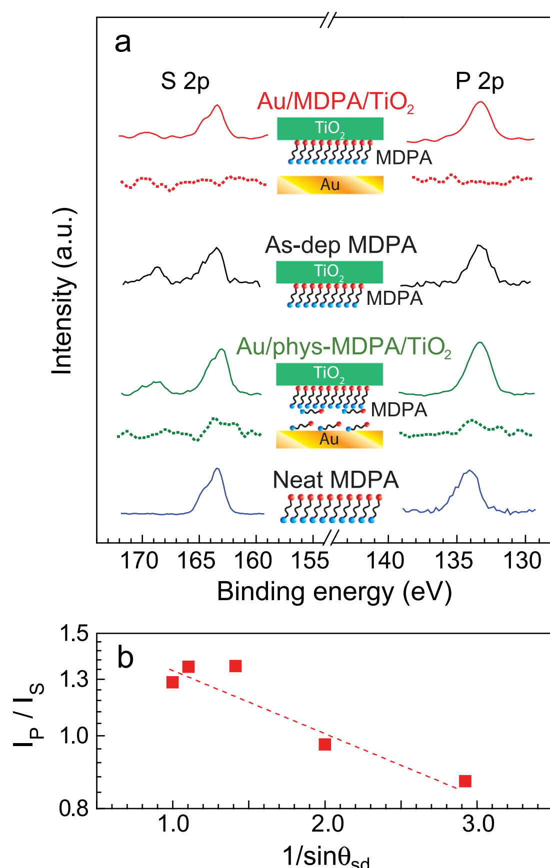

FIG. 2. (a) Core-level S 2p and P 2p bands from TiO_2 (solid lines) and Au (dotted lines) fracture surfaces for Au/MDPA/TiO_2 structures, with (green) and without (red) physisorbed MDPA. Baseline spectra from as-prepared MDPA NML on TiO_2 (black) and neat MDPA powder (blue) are shown for comparison. (b) P 2p: S 2p integrated intensity ratio I_P/I_S for MDPA as a function of decreasing sample surface-detector takeoff angle θ_{sd}. The dashed line shows a semi-log fit of the intensity ratio.

stronger than bonds at untreated Au/TiO_2 interfaces. This conclusion is further supported by $< \sim 1$ at. % traces of Au on the titania fracture surface of Au/MDPA/TiO_2 structures (Fig. 3), not seen on that of pristine Au/TiO_2 interfaces.

Our experimental results lead us to conclude that MDPA bonding with Au and TiO_2 through P-O-Ti and Au-S bridges are key to interface toughening, which correlates with the increased interfacial thermal conductance.[11] The lack of formation of even one of these bridges weakens the interface, as corroborated by the lower Γ_c for Au/MDPA/TiO_2 interfaces having remnant physisorbed MDPA (phys-MDPA) in addition to the MDPA NML that is chemically anchored to TiO_2. Au fracture surfaces of interfaces with phys-MDPA exhibit both S 2p and P 2p signatures, unlike interfaces with purely chemisorbed MDPA NML on TiO_2 (Fig. 2(a)). This result shows that some of the remnant physisorbed MDPA molecules chemically bond with the Au overlayer, but are obstructed from bonding with titania by the chemisorbed MDPA NML. Thus, the NML must bond with both materials simultaneously to fully realize interface toughening and thermal conductance enhancement.

Our experimental results showing Au-S scission to be the fracture pathway is consistent with the diatomic bond dissociation energies[26] relevant to the Au/MDPA/TiO_2 interface. In particular, the 2.7 eV diatomic Au-S bond is the weakest of all possible bonds at the interface: Ti-O (7.3 eV), P-O (6.5 eV), C-P (5.4 eV), C-C (6.3 eV), and C-S (7.5 eV). Our DFT calculations of cleavage energies also indicate that fracture will most likely occur at the Au/MDPA interface rather than at the TiO_2/MDPA interface or midway through MDPA (Fig. 4). However, a deeper inspection of the DFT calculations indicates that S-C bond is weaker than the Au-S bond. This difference is not entirely unexpected because our calculations do not account for factors that may alter the Au-S bond strength. For instance, oxidation of mercaptan to sulfonate/sulfonic acid[27] moieties, or disulfide bond formation may impact the Au-S bond energy by influencing the lateral interactions between adjacent MDPA molecules in the nanolayer. DFT calculations showing the shifting of the weak link from the Au-S bond to the S-C bond near the Au-MDPA interface at higher MDPA coverages support this hypothesis. Notwithstanding such factors, and environmentally related uncertainties, our simulations and experiments concur that fracture occurs in the vicinity of the Au/MDPA interface.

Implicit in the above results is that the phosphonic acid-titania bonds are strong and insensitive to moisture[17] unlike pristine or organosilane-tailored metal-ceramic interfaces.[28,29] For instance, Cu-silica interfaces modified with a

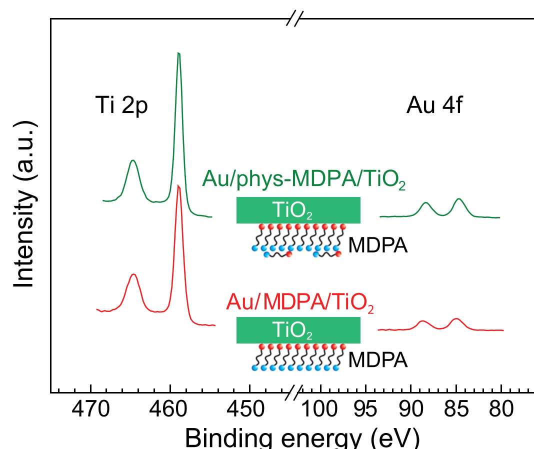

FIG. 3. Traces of Au seen on TiO_2 fracture surfaces from structures with (green) and without (red) physisorbed MDPA.

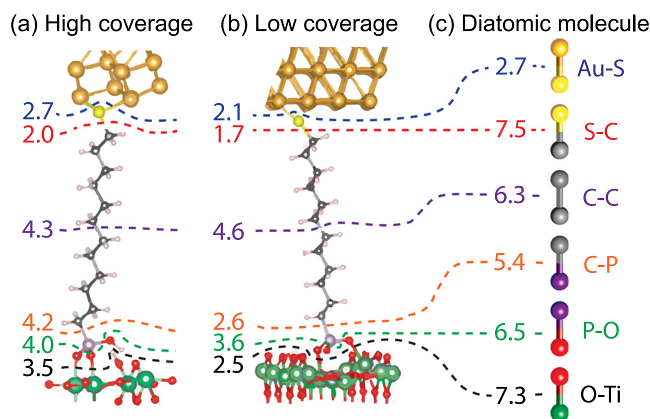

FIG. 4. Schematic sketches showing results of DFT calculations of bond cleavage energies of MDPA-functionalized Au-TiO_2 interfaces for (a) high coverage (b) low coverage, and for (c) the diatomic molecules. The bond energies in eV are shown adjacent to dashed lines denoting cleavage locations considered in our study.

Downloaded 13 Jun 2013 to 137.99.20.247. This article is copyrighted as indicated in the abstract. Reuse of AIP content is subject to the terms at: http://apl.aip.org/about/rights_and_permissions

mercaptopropyltrimethoxysilane (MPTMS) NML delaminate by the scission of 8.3 eV Si-O bonds due to moisture-weakening, while 2.8 eV Cu-S bonds remain intact.[6] It is unclear why Au-S bonds break at Au/MDPA/TiO_2 interfaces at $\Gamma_c = 2.6\ Jm^{-2}$ while Cu-S bonds remain intact even at $\Gamma_c = 9.1\ Jm^{-2}$ for Cu/MPTMS/SiO_2 interfaces. Further studies are needed to develop a theoretical framework to understand quantitative correlations between thermodynamic bond energies and fracture toughness across multiple materials systems.

In summary, we have demonstrated the use of a mercaptan-terminated organophosphonate nanomolecular layer to obtain two- to three-fold increase in interfacial fracture toughness and thermal conductance of gold-titania interfaces. Electron spectroscopy shows that observed enhancements are due to strong Au-S and P-O-Ti bonds at Au/MDPA and MDPA/TiO_2 interfaces, respectively. Fracture surface analysis and density functional theory calculations indicate that Au/MDPA/TiO_2 interfaces delaminate in the vicinity of Au-S bonds and that MDPA/TiO_2 interfaces are resilient to moisture attack. Our results, and the versatility of phosphonates as surface functionalization agents for technologically relevant substrates, unlock uncharted avenues for molecular engineering multiple interfacial properties in materials and devices for a variety of applications.

We gratefully acknowledge funding support from a National Science Foundation awards CMMI 1100933/926 and ECCS 1002282/301. P.H.M. acknowledges support from the Partner University Fund in which both RPI and Université de Montpellier 2 are partners.

[1]P. Kim, S. C. Jones, P. J. Hotchkiss, J. N. Haddock, B. Kippelen, S. R. Marder, and J. W. Perry, Adv. Mater. **19**, 1001 (2007).
[2]J. Robertson, Rep. Prog. Phys. **69**, 327 (2006).
[3]G. D. Wilk, R. M. Wallace, and J. M. Anthony, J. Appl. Phys. **89**, 5243 (2001).
[4]A. Wold, Chem. Mater. **5**, 280 (1993).
[5]J. Amalric, P. H. Mutin, G. Guerrero, A. Ponche, A. Sotto, and J.-P. Lavigne, J. Mater. Chem. **19**, 141 (2009).
[6]D. D. Gandhi, M. Lane, Y. Zhou, A. P. Singh, S. Nayak, U. Tisch, M. Eizenberg, and G. Ramanath, Nature **447**, 299 (2007).
[7]G. Ramanath, J. R. A. Carlsson, J. E. Greene, L. H. Allen, V. C. Hornback, and D. J. Allman, Appl. Phys. Lett. **69**, 3179 (1996).
[8]G. Ramanath, G. Cui, P. G. Ganesan, X. Guo, A. V. Ellis, M. Stukowski, K. Vijayamohanan, P. Doppelt, and M. Lane, Appl. Phys. Lett. **83**, 383 (2003).
[9]Y. Selzer and D. Cahen, Adv. Mater. **13**, 508 (2001).
[10]D. O. Hutchins, O. Acton, T. Weidner, N. Cernetic, J. E. Baio, G. Ting, D. G. Castner, H. Ma, and A. K.-Y. Jen, Org. Electron. **13**, 464 (2012).
[11]P. J. O'Brien, S. Shenogin, J. Liu, P. K. Chow, D. Laurencin, P. H. Mutin, M. Yamaguchi, P. Keblinski, and G. Ramanath, Nature Mater. **12**, 118 (2013).
[12]G. Guerrero, P. H. Mutin, and A. Vioux, Chem. Mater. **13**, 4367 (2001).
[13]O. Acton, G. Ting, H. Ma, J. W. Ka, H. Yip, N. M. Tucker, and A. K. Y. Jen, Adv. Mater. **20**, 3697 (2008).
[14]S. Marcinko and A. Fadeev, Langmuir **20**, 2270 (2004).
[15]J. Randon, J. Membr. Sci. **98**, 119 (1995).
[16]P. Bonhote, J. E. Moser, R. Humphry-Baker, N. Vlachopoulos, S. M. Zakeeruddin, L. Walder, and M. Gratzel, J. Am. Chem. Soc. **121**, 1324 (1999).
[17]P. H. Mutin, G. Guerrero, and A. Vioux, J. Mater. Chem. **15**, 3761 (2005).
[18]S. Garg, R. Teki, M. W. Lane, and G. Ramanath, Appl. Phys. Lett. **99**, 133101 (2011).
[19]B. Singh, S. Garg, J. Rathore, R. Moore, N. Ravishankar, L. Interrante, and G. Ramanath, ACS Appl. Mater. Interfaces **2**, 1275 (2010).
[20]R. H. Dauskardt, M. Lane, Q. Ma, and N. Krishna, Eng. Fract. Mech. **61**, 141 (1998).
[21]G. Eesley, Phys. Rev. B **33**, 2144 (1986).
[22]M. Polcik, L. Wilde, J. Haase, B. Brena, G. Comelli, and G. Paolucci, Surf. Sci. **381**, L568 (1997).
[23]G. Kresse and J. Furthmuller, Phys. Rev. B **54**, 11169 (1996).
[24]J. P. Perdew, J. A. Chevary, S. H. Vosko, K. A. Jackson, M. R. Pederson, D. J. Singh, and C. Fiolhais, Phys. Rev. B **46**, 6671 (1992).
[25]P. E. Blochl, Phys. Rev. B **50**, 17953 (1994); G. Kresse and D. Joubert, *ibid.* **59**, 1758 (1999).
[26]*CRC Handbook of Chemistry and Physics*, 93rd ed., edited by W. M. Haynes (CRC Press, 2012).
[27]P. G. Ganesan, A. Kumar, and G. Ramanath, Appl. Phys. Lett. **87**, 011905 (2005).
[28]A. Jain, B. Singh, S. Garg, N. Ravishankar, M. Lane, and G. Ramanath, Phys. Rev. B **83**, 035412 (2011).
[29]D. Vijayashankar, H. Zhu, S. Garg, R. Teki, R. Ramprasad, M. W. Lane, and G. Ramanath, Appl. Phys. Lett. **99**, 133103 (2011).

Downloaded 13 Jun 2013 to 137.99.20.247. This article is copyrighted as indicated in the abstract. Reuse of AIP content is subject to the terms at: http://apl.aip.org/about/rights_and_permissions